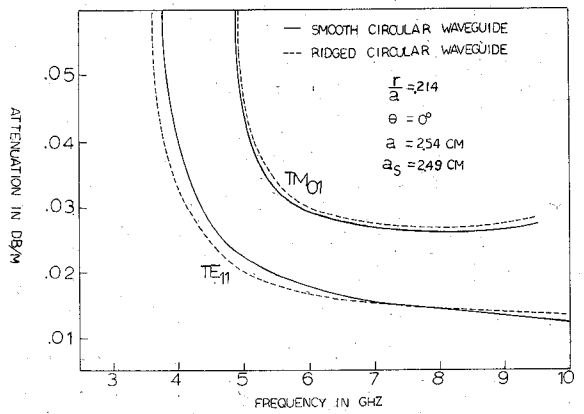

Fig. 3. Attenuation of TE_{11} and TM_{01} waves versus frequency.

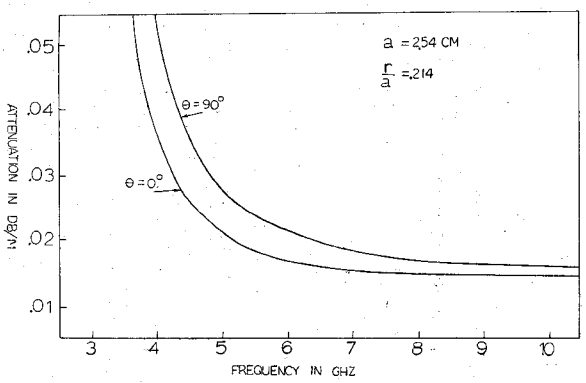

Fig. 4. Comparison of attenuation of TE_{11} wave for $\theta = 0°$ and $\theta = 90°$.

Conclusion

The cutoff frequencies and attenuation of waves in a ridged circular waveguide are calculated. The results suggest that a ridged circular waveguide has a lower loss and larger bandwidth than those of a smooth circular waveguide for the dominant TE_{11} wave polarized in ridge-pair plane in the normal operating band. Attentuation of TE_{11} wave in a ridged circular waveguide is minimum when the wave is polarized in the ridge-pair plane ($\theta = 0°$) and is maximum when the wave is polarized normal to the ridge-pair plane ($\theta = 90°$).

Conclusions reached here are drawn from the calculations of a formulation based on perturbation theory. The results do not hold for large r/a, however. Since the exact field distribution within the waveguide is unknown, error can only be estimated. For design purposes, however, the error can be estimated for a fixed r/a on the basis of a comparison between (1) and the more exact solutions [4], [5] for a rectangular waveguide with a same wall-deformation. For example, the cutoff frequency-shift based on (1) is calculated in a rectangular waveguide with a rectangular longitudinal ridge attached in the H plane with dimensions corresponding to $r/a = 0.275$ in Fig. 2. The result is then compared to that of Cohn's work [4] and an error is obtained. If this same error is assumed for the case of ridged circular guide, then the cutoff frequency-shift is estimated to be within 0.65 percent for TE_{11} mode and 0.77 percent for TM_{01} mode. For a circular ridge which is the case in this study, the result is expected to be somewhat better, because of the smoothness of the wall-boundary, although a complete error analysis for the wide range of r/a in Figs. 2–4 has not been carried out.

References

[1] T. Charlton, Andrew Corporation, Orland Park, Ill., private communication, Jan. 1970.
[2] R. F. Harrington, *Time Harmonic Electromagnetic Fields*. New York: McGraw-Hill, 1961, p. 327.
[3] S. Ramo and J. R. Whinnery, *Fields and Waves in Modern Radio*. New York: Wiley, 1965, p. 405.
[4] S. B. Cohn, "Properties of ridged wave guide," *Proc. IRE*, vol. 35, pp. 783–788, Aug. 1947.
[5] E. V. Juhl, W. J. Bleackley, and M. M. Steen, "The design of waveguides with symmetrically placed double ridges," *IEEE Trans. Microwave Theory Tech.*, vol. MTT-17, pp. 397–399, July 1969.

Magnetostatic Surface Waves in Ferrite Slab Adjacent to Semiconductor

MASAMITSU MASUDA, MEMBER, IEEE, NION S. CHANG, MEMBER, IEEE, AND YUKITO MATSUO

***Abstract*—Magnetostatic surface waves propagating along the ferrite slab adjacent to a semiconductor are discussed in this paper. Our numerical results indicate that the conductivity of the semiconductor plays an important role in the determination of the dispersion relation in the case of nondrifting carriers. The backward wave appears for a finite value of the conductivity.**

I. Introduction

Magnetostatic modes propagating along a ferromagnetic slab in free space were first examined by Damon and Eshbach [1] (DE waves). Applying a dc magnetic field transverse to the direction of the wave propagation, the surface wave which corresponds to the $\theta = 90°$ spin wave is excited. This wave is unique to the slab configuration. Seshadri [2] considered the case where a metal conductor was placed on one face of the slab. Such a grounded ferrite slab has two different surface waves which propagate in opposite direction to each other. Both surface waves are forward modes. Subsequently, Bongianni [3] discussed magnetostatic waves in the dielectric-layered structure where the dielectric material was between a YIG film and a perfect conductor. A backward wave appears at some value of the thickness of the dielectric layer. On the other hand, the general theory of the surface wave on a metallized ferrite film, including dipolar, exchange, and conductivity effects, has been treated by Wolfram and DeWames [4].

Our interest is not only in the behavior of the magnetostatic waves but also in the wave interaction between the ferrite and the semiconductor. It has been suggested that the solid-state traveling wave amplifier (STWA) can be constructed with a layered structure containing both materials [5]–[7]. A detailed understanding of the coupling of the spin wave in ferrite and the carrier wave in semiconductor is important for the design of STWA. Preliminary to a discussion of the amplification process, we deal in the present paper with the magnetostatic surface waves propagating along a ferrite slab adjacent to a semiconductor. The finite conductivity of the semiconductor gives us remarkable changes to the properties of the surface waves. The dispersion relationship can be obtained by solving the boundary value problem for three regions of ferrite, semiconductor, and free space.

II. Analysis

The geometry treated in this paper is a layered structure constituted by a ferrite slab and a semiconductor layer in free space, as shown in Fig. 1. The external dc magnetic field is applied parallel to the y direction. The propagating directions of magnetostatic surface waves and the carrier flow in the semiconductor are chosen to be in the z direction. Our two-dimensional analysis is based on the assumptions that the wave varies as $\exp j(\omega t - \beta z)$ and that all properties are independent of y ($\partial/\partial y = 0$).

The field components in the semiconductor region, which is a collision-dominated system for electrons, satisfy the following equations:

$$\nabla \times \boldsymbol{H} = \boldsymbol{J} + j\omega\epsilon_s \boldsymbol{E} \tag{1}$$

$$\nabla \times \boldsymbol{E} = -j\omega\mu_0 \boldsymbol{H} \tag{2}$$

$$\nabla \times \boldsymbol{E} = \rho/\epsilon_s \tag{3}$$

$$\boldsymbol{J} = \rho_0 \boldsymbol{V} + \rho \boldsymbol{V}_0 \tag{4}$$

$$\boldsymbol{V} = \bar{\mu}_s(\boldsymbol{E} + \boldsymbol{V} \times \boldsymbol{B}_0 + \boldsymbol{V}_0 \times \boldsymbol{B}) \tag{5}$$

$$\bar{\mu}_s = \begin{vmatrix} \mu_t & 0 & 0 \\ 0 & \mu_t & 0 \\ 0 & 0 & \mu_z \end{vmatrix}, \qquad \mu_t = v/E, \quad \mu_z = \partial v/\partial E \tag{6}$$

Manuscript received March 5, 1973; revised September 17, 1973.
The authors are with the Institute of Scientific and Industrial Reseach, Osaka University, Osaka, Japan.

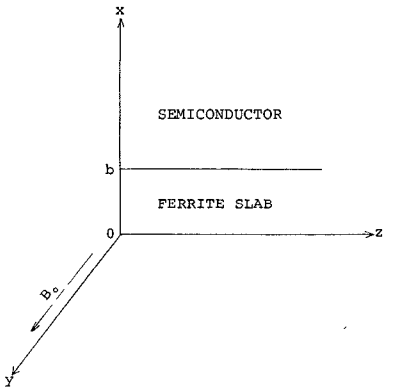

Fig. 1. Geometry for our analysis.

where ϵ_s is the permittivity of semiconductor and $\bar{\mu}_s$ is the tensor of electron mobility; however, $\mu_t = \mu_z = v/E$ in the isotropic medium such as InSb. Subscript 1 which usually denotes RF quantities is omitted, but subscript 0 refers to dc quantities.

The invariance of the fields in the y direction leads to two uncoupled waves: one has the field components E_x, E_z, and H_y (TM-mode) and the other has H_x, H_z, and E_y (TE-mode). The former is the longitudinal space charge wave modified by the dc magnetic field. In considering the effect of the magnetic field for Gunn-effect domain formation, the TM-mode is important. The latter wave is regarded as a kind of carrier wave which is described by the next equations:

$$\frac{\partial^2 E_y}{\partial x^2} - \gamma_s^2 E_y = 0 \tag{7}$$

$$\gamma_s^2 = \beta^2 - k_s^2\left\{1 - j\frac{\beta_{ct}}{\beta_0}\left(1 - \frac{\beta}{\beta_0}\right)\right\} \tag{8}$$

$$B_x = -\left(\frac{\beta}{\omega}\right)E_y \tag{9}$$

$$H_z = j\left(\frac{1}{\mu_0\omega}\right)\frac{\partial E_y}{\partial x} \tag{10}$$

where $\beta_0 = \omega/v_0$, $\beta_{ct} = \rho_0\mu_t/\epsilon_s v_0$, and $K_s^2 = \omega^2\epsilon_s\mu_0$.

From the same two-dimensional analysis applied to the ferrite region, it is evident that the wave due to the precession of spins in the ferrite has the components H_x, H_z, and E_y, as generally known. Therefore, the TE-mode must be chosen in the semiconductor. From (7)

$$E_y = C_1 e^{-\gamma_s x}. \tag{11}$$

When the wavenumber β ranges over $10 < \beta < 10^5$ cm^{-1}, the quasi-static approximation is valid. The TE-mode obtained from the two-dimensional analysis in ferrite and free-space regions corresponds to the magnetostatic surface modes. Considering the lossless ferrite slab, the relative permeability tensor $\bar{\mu}_f$ is

$$\bar{\mu}_f = \begin{vmatrix} \mu_1 & 0 & -j\mu_2 \\ 0 & 1 & 0 \\ j\mu_2 & 0 & \mu_1 \end{vmatrix} \tag{12}$$

$$\mu_1 = 1 + \frac{\omega_r\omega_M}{\omega_r^2 - \omega^2} \quad \mu_2 = \frac{\omega\omega_M}{\omega_r^2 - \omega^2} \quad \omega_r = \gamma H_i \quad \omega_M = \gamma\cdot 4\pi M_s \tag{13}$$

where H_i is the internal dc magnetic field, $4\pi M_s$ the saturation magnetization, and γ the gyromagnetic ratio. The RF magnetic field can be described as the gradient of a magnetic scalar potential ϕ.

$$\boldsymbol{H} = -\nabla\phi \tag{14}$$

$$\nabla\cdot\boldsymbol{B} = 0 \tag{15}$$

$$\boldsymbol{B} = \mu_0\bar{\mu}_f\boldsymbol{H}. \tag{16}$$

From (12), (14)–(16),

$$\frac{\partial^2\phi}{\partial x^2} - \beta^2\phi = 0. \tag{17}$$

The following expression for ϕ, H_z, and B_x in each region can be derived from the above equations. For $0 \le x \le b$ in ferrite,

$$\phi = C_2 e^{|\beta|x} + C_3 e^{-|\beta|x} \tag{18a}$$

$$H_z = j\beta\phi = j\beta(C_2 e^{|\beta|x} + C_3 e^{-|\beta|x}) \tag{18b}$$

$$B_2 = \mu_0(\mu_1 H_x - j\mu_2 H_z)$$
$$= \mu_0\{C_2 e^{|\beta|x}(\mu_1|\beta| - \mu_2\beta) - C_3 e^{-|\beta|x}(\mu_1|\beta| + \mu_2\beta)\}. \tag{18c}$$

For $x \le 0$ in free space,

$$\phi = C_4 e^{|\beta|x} \tag{19a}$$

$$H_z = j\beta C_4 e^{|\beta|x} \tag{19b}$$

$$B_x = -\mu_0|\beta|C_4 e^{|\beta|x}. \tag{19c}$$

Applying the boundary conditions that both H_z and B_x are continuous at each interface and eliminating C_1, C_2, C_3, and C_4 from the related equations, we can obtain the following dispersion relation:

$$e^{2|\beta|b} = \frac{\{(\mu_1 + \mu_2 s)\gamma_s' - 1\}(\mu_1 - \mu_2 s - 1)}{\{(\mu_1 - \mu_2 s)\gamma_s' + 1\}(\mu_1 + \mu_2 s + 1)} \tag{20}$$

where $s = \beta/|\beta|$ and $\gamma_s' = \gamma_s/|\beta|$. As the wave propagates along either $+z$ or $-z$ direction, s takes on the value $+1$ or -1. Considering that $|\beta^2| \gg k_s^2$ is reasonable in the semiconductor, the approximated equation for γ_s' can be obtained from (8):

$$\gamma_s'^2 \simeq 1 + j\frac{\mu_0\sigma}{\beta^2}(\omega - |\beta|v_0) \tag{21}$$

where σ is the conductivity.

Equations (20), (21), and (13) yield the following polynomial expression for the normalized angular frequency $F(=\omega/\omega_r)$:

$$g(F) = T_5F^5 + T_4F^4 + T_3F^3 + T_2F^2 + T_1F + T_0 \tag{22}$$

where

$$T_5 = j\frac{\mu_0\sigma\omega_r b^2}{(|\beta|b)^2}4e^{4|\beta|b}$$

$$T_4 = j\frac{\mu_0\sigma\omega_r b^2}{(|\beta|b)^2}4e^{2|\beta|b}\left\{Gs(e^{2|\beta|b} - 1) - (|\beta|b)\left(\frac{\omega_r b}{v_0}\right)^{-1}e^{2|\beta|b}\right\}$$

$$T_3 = 8Gse^{2|\beta|b}(e^{2|\beta|b} - 1) - j\frac{\mu_0\sigma\omega_r b^2}{(|\beta|b)^2}\Bigg[G^2(e^{2|\beta|b} - 1)^2$$
$$- 4e^{2|\beta|b}\Bigg[(1 + G)\{e^{2|\beta|b}(2 + G) - G\}$$
$$+ (|\beta|b)\left(\frac{\omega_r b}{v_0}\right)^{-1}Gs(e^{2|\beta|b} - 1)\Bigg]\Bigg]$$

$$T_2 = -4e^{2|\beta|b}(e^{2|\beta|b} - 1)G(2 + G) - j\frac{\mu_0\sigma\omega_r b^2}{(|\beta|b)^2}\Bigg[2Gs(e^{2|\beta|b} - 1)$$
$$\times (1 + G)\{e^{2|\beta|b}(2 + G) - G\} + (|\beta|b)\left(\frac{\omega_r b}{v_0}\right)^{-1}[G^2(e^{2|\beta|b} - 1)^2$$
$$- 4e^{2|\beta|b}(1 + G)\{e^{2|\beta|b}(2 + G) - G\}]\Bigg]$$

$$T_1 = -2Gs(e^{2|\beta|b} - 1)\{e^{2|\beta|b}(2 + G)^2 - G^2\} + j\frac{\mu_0\sigma\omega_r b^2}{(|\beta|b)^2}$$
$$\times (1 + G)\{e^{2|\beta|b}(2 + G) - G\}\Bigg[(1 + G)\{e^{2|\beta|b}(2 + G) - G\}$$
$$+ 2(|\beta|b)\left(\frac{\omega_r b}{v_0}\right)^{-1}Gs(e^{2|\beta|b} - 1)\Bigg]$$

$$T_0 = (1 + G)^2\{e^{2|\beta|b}(2 + G) - G\}^2 - \{2e^{2|\beta|b} + G(e^{2|\beta|b} + 1)\}^2$$
$$- j\frac{\mu_0\sigma\omega_r b^2}{(|\beta|b)^2}(|\beta|b)\left(\frac{\omega_r b}{v_0}\right)^{-1}(1 + G)^2\{e^{2|\beta|b}(2 + G) - G\}^2 \tag{23}$$

and $G = \omega_M/\omega_r$.

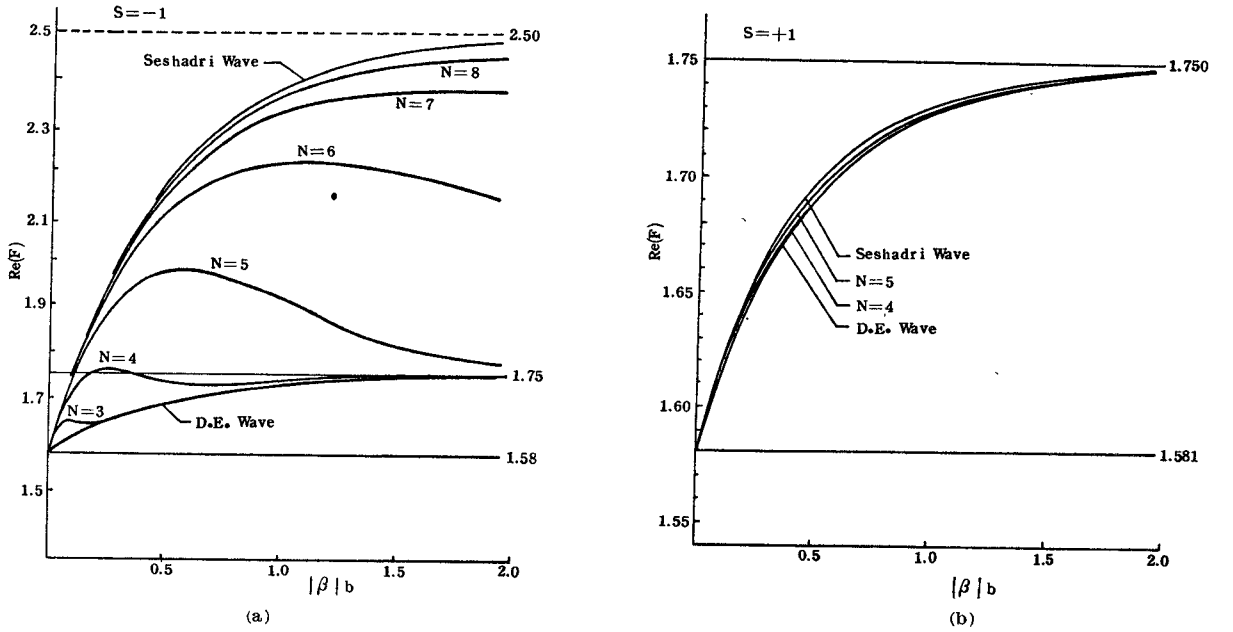

Fig. 2. Re $(F) - |\beta| b$ diagrams, where the conductivity is variable, $H_i = 400$ Oe, $4\pi M_s = 600$ G, and $b = 100\ \mu$m. (a) For $s = -1$. (b) For $s = +1$.

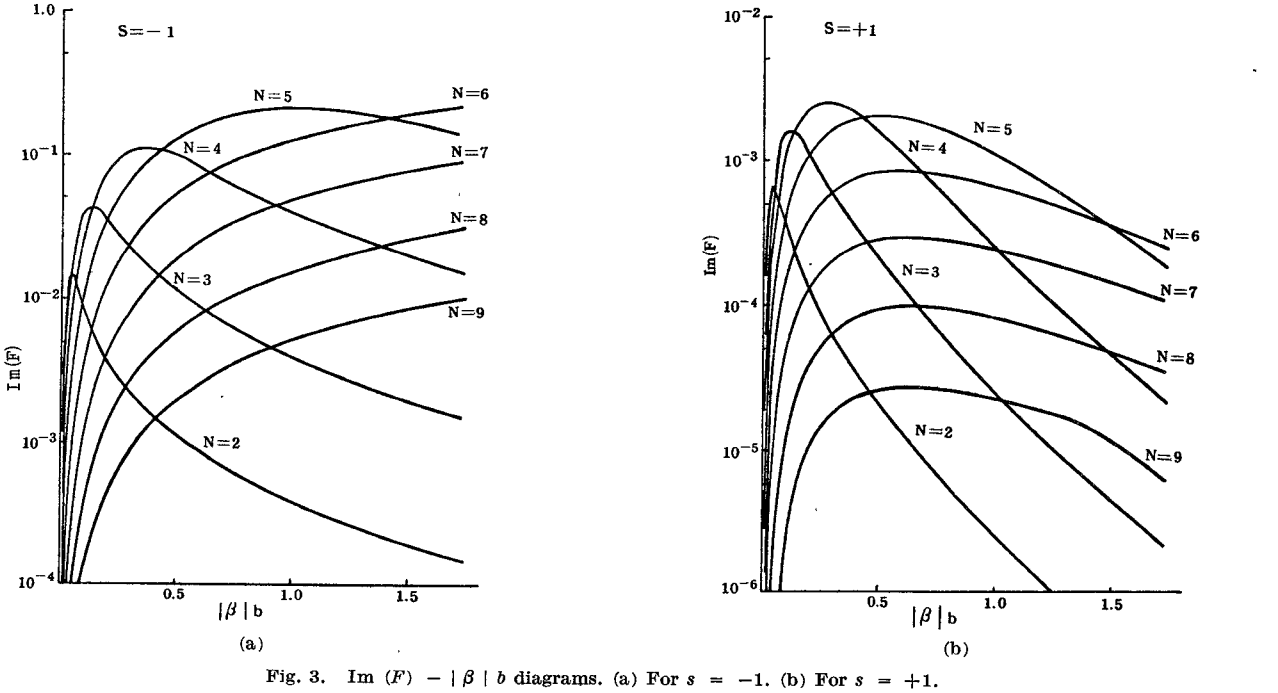

Fig. 3. Im $(F) - |\beta| b$ diagrams. (a) For $s = -1$. (b) For $s = +1$.

The equation that $g(F) = 0$ may have five complex roots of F for some value of β, but it is our purpose to elucidate the behavior of the magnetostatic surface wave propagating along the ferrite slab adjacent to the semiconductor. In order to obtain the asymptotic solutions for (22), the Newton–Raphson method in a complex region was applied to our computer computation. A pair of solutions $(F_0, |\beta|b)$ for the DE wave were chosen as the initial value, where F_0 is real.

III. Results and Discussion

It can be predicted from (23) that the factor commonly contained in all coefficients, which is $\mu_0\sigma\omega_r b$, exerts a crucial influence on the dispersion relation. With respect to constant values of ω_r and b, we examined how the properties of a magnetostatic surface wave was modulated by the conductivity of a semiconductor in the absence of a bias voltage ($v_0 = 0$).

The diagrams of Re $(F) - |\beta|b$ obtained from our computer computation are sketched in Fig. 2. The parameter N which implies the variation of the conductivity satisfies the next relation:

$$\sigma = en_0\mu_t = e \times 10^{(N+18)}\ \text{mho/m} \tag{24}$$

where e is the electronic charge and n_0 the doping density. The application of n-InSb at 77 K realizes the situation at $N = 4$ or 5, for example $n_0 = 10^{16\sim17}$ cm^{-3} and $\mu_t = 10^4$ cm^2/V·s. At $N = 3$, it may be possible to use n-GaAs in room temperature. In $N \geq 6$, it is necessary to use the heavily doped semiconductor which is more metallic.

As is evident from Fig. 2(a) and (b), the propagation characteristics for $-z$ direction are different from those for $+z$ direction. This phenomenon is dependent on whether the magnetostatic surface wave propagates along the plane at $x = b$ or $x = 0$. For $s = -1$, since the magnetic potential distribution is concentrated at the interface between the ferrite slab and the semiconductor, the surface wave is particularly sensitive to the conductivity. Both the DE wave

and the Seshadri wave in the limiting cases of our theory are forward waves; however, the finite conductivity of the semiconductor makes it possible to excite backward waves. When the conductivity is increased, the discrepancy from the DE wave is first larger in smaller wavenumber and the passband becomes broader. At $N = 4$, the dispersion curve can cross over the upper bound of the frequency spectrum for the DE wave. As it approaches to the Seshadri wave, the characteristic of the backward wave disappears gradually. On the other hand, in the case of $s = +1$ where the surface wave propagates along the interface at $x = 0$, no remarkable changes of the properties can be observed [Fig. 2(b)] and this wave is similar to the DE wave.

The diagrams of Im $(F) - |\beta|$ as shown in Fig. 3 offer the information about the attenuation for the surface wave. Significant interaction between the surface wave and the electrons in the semiconductor is expected. In the absence of a bias voltage, this interaction can be regarded as the dominant cause of loss for the surface wave over the range $1 \leq N \leq 5$. Furthermore, the higher conductivity makes the semiconductor so metallic that the well-known skin effect may play an important role at $N \geq 6$. Fig. 3 implies that the optimum coupling of spins and electrons can be attained in the neighborhood of $N = 5$. In the presence of drifting carriers in the semiconductor, the wave interaction leads to the creation of the growing wave. It is natural that the loss for $s = +1$ is less than that for $s = -1$ by about -20 dB.

IV. Conclusion

The magnetostatic surface waves in the ferrite slab adjacent to the semiconductor have been investigated in the previous sections. Our analytical results have pointed out that the propagation characteristics of the surface wave are affected considerably by the finite conductivity of the semiconductor in the absence of bias voltage. In particular the backward waves are excited. It is believed that optimum coupling of spins and electrons is attained in the neighborhood of $N = 5$. If drifting carriers are present in the semiconductor, it is anticipated that the wave interaction will result in a growing wave, thereby providing gain. In addition, it may be possible to construct a voltage-tuned delay line by utilizing the composite structure constituted of YIG-film and the semiconductor.

References

[1] R. W. Damon and J. R. Eshbach, "Magnetostatic modes of a ferromagnetic slab," *J. Appl. Phys.* (supplement to vol. 31), pp. 104s–105s, May 1960.
[2] S. R. Seshadri, "Surface magnetostatic modes of a ferrite slab," *Proc. IEEE*, vol. 58, pp. 506–507, Mar. 1970.
[3] W. L. Bongianni, "Magnetostatic propagation in a dielectric layered structure," *J. Appl. Phys.*, vol. 43, pp. 2541–2548, June 1972.
[4] T. Wolfram and R. E. DeWames, "Dipole-exchange surface wave dispersion and loss for a metalized ferrite film," *J. Phys. (Paris)* (Colloque C1, Supplement to nos. 2–3, vol. 32, pp. 1171–1173, Feb.–Mar. 1971.
[5] B. B. Robinson, B. Vural, and J. P. Parekh, "Spin-wave/carrier-wave interaction," *IEEE Trans. Electron Devices*, vol. ED-17, pp. 224–229, Mar. 1970.
[6] E. Schlömann, "Amplification of magnetostatic surface waves by interaction with drifting carriers in crossed electric and magnetic fields," *J. Appl. Phys.*, vol. 40, pp. 1422–1423, Mar. 1969.
[7] N. S. Chang and Y. Matsuo, "Possibility of utilizing the coupling between a backward wave in YIG and waves associated with drift carrier stream in semiconductor," *Proc. IEEE*, vol. 56, pp. 765–766, Apr. 1968.

Coupled-Mode Analysis of Longitudinally Magnetized Ferrite Phase Shifters

W. E. HORD, MEMBER, IEEE, AND F. J. ROSENBAUM, SENIOR MEMBER, IEEE

***Abstract*—Application of a coupled-mode formalism to longitudinally magnetized ferrite phase shifters provides an explanation of the increase or decrease of insertion phase with increasing magnetization which is observed in different types of phase shifters. If the higher order mode is TM, the phase shift increases with magnetization while the reverse happens if the higher order mode is TE.**

The generalized telegraphists' equations are used to analyze the TEM phase shifter. The maximum phase shift that can be obtained is determined by the effective permeability of the ferrite. However, coupling to higher order cutoff modes reduces the phase shift significantly.

Manuscript received March 28, 1973; revised August 31, 1973. This work was supported in part by a subcontract from the Monsanto Research Corporation, Dayton, Ohio, under Contract F33615-72-C-1034, from the Air Force Avionics Laboratory, Wright-Patterson Air Force Base, Dayton, Ohio.

W. E. Hord is with the Department of Engineering, Southern Illinois University, Edwardsville, Ill. 62025.
F. J. Rosenbaum is with the Department of Electrical Engineering, Washington University, St. Louis, Mo. 63130.

I. Introduction

In their classic paper Suhl and Walker [1] examined propagation in a ferrite-filled coaxial waveguide magnetized to saturation along the direction of propagation. They showed that, if the spacing between inner and outer conductors was sufficiently small, for the dominant (quasi-TEM) mode the ferrite could be represented as an isotropic lossless medium with an effective permeability given by

$$\mu_{\text{eff}} = \frac{\mu^2 - \kappa^2}{\mu} \tag{1a}$$

where

$$\mu = 1 + \frac{\omega_0 \omega_m}{\omega_0^2 - \omega^2} \tag{1b}$$

and

$$\kappa = \frac{\omega \omega_m}{\omega_0^2 - \omega^2} \tag{1c}$$

are the elements of the Polder tensor [2]

$$\bar{\bar{\mu}} = \mu_0 \begin{bmatrix} \mu & -j\kappa & 0 \\ j\kappa & \mu & 0 \\ 0 & 0 & 1 \end{bmatrix} \tag{2}$$

with

$$\omega_m = (2\pi\gamma)(4\pi M_s)$$

$$\omega_0 = (2\pi\gamma) H_0$$

where

ω	microwave radian frequency;
$4\pi M_s$	ferrite saturation magnetization;
H_0	external dc magnetic field;
γ	2.8 MHz/Oe;
μ_0	permeability of free space equals $4\pi \times 10^{-7}$ H/m.

Through symmetry arguments they also showed that the same result was valid for propagation in a longitudinally magnetized ferrite contained between perfectly conducting parallel planes, in the limit of small spacing between the planes.

In this paper, longitudinally magnetized ferrites in guided wave structures are examined. Coupled-mode theory is employed to gain insight into the general characteristics of such structures. A detailed analysis of the TEM phase shifter is undertaken to examine the variation of effective permeability and hence, phase shift, with plate spacing.

II. Coupled-Mode Theory

In this section we describe how differential phase shift is obtained in longitudinally magnetized ferrite structures. We approach the problem from the viewpoint of mode coupling between the dominant mode and cutoff modes capable of storing electromagnetic energy. This type of analysis has successfully predicted the behavior of the Faraday rotation phase shifter [3] and is the only plausible explanation of the Reggia–Spencer phase shifter [4]–[6].

Since the anisotropy of (2) exists only in the transverse plane, we may define a transverse tensor permeability as

$$\bar{\bar{\mu}}_t = \mu_0 \begin{bmatrix} \mu & -j\kappa \\ j\kappa & \mu \end{bmatrix}. \tag{3}$$

Now consider two transmission lines which are nonreciprocally coupled by this medium. If V_1 and I_1 represent the uncoupled volt-